

Moiré Insulators viewed as the Surface of three dimensional Symmetry Protected Topological Phases

Chao-Ming Jian^{1,2} and Cenke Xu³

¹*Kavli Institute of Theoretical Physics, Santa Barbara, CA 93106, USA*

²*Station Q, Microsoft Research, Santa Barbara, California 93106-6105, USA*

³*Department of Physics, University of California, Santa Barbara, CA 93106, USA*

Recently, correlated physics such as superconductivity and insulator at commensurate fractional electron fillings has been discovered in several different systems with Moiré superlattice and narrow electron bands near charge neutrality. Before we learn more experimental details and the accurate microscopic models describing the insulators, some general conclusions can already be made about these systems, simply based on their symmetries and electron fillings. The insulator in the Moiré superlattice is described by an effective spin-orbital model with approximate higher symmetries than ordinary spin systems. We demonstrate that both the insulators observed at the 1/2 and 1/4 fillings away from the charge neutrality can be viewed as the boundary of a three dimensional bosonic symmetry protected topological phase, and hence have the 't Hooft anomaly once the spatial symmetries are viewed as internal symmetries.

PACS numbers:

I. INTRODUCTION

The Lieb-Schultz-Mattis (LSM) theorem¹, and its higher dimensional generalizations^{2,3} state that if a quantum spin system defined on a lattice has odd number of spin-1/2s per unit cell, then any local spin Hamiltonian which preserves the spin and translation symmetry, cannot have a featureless (gapped and nondegenerate) ground state. A system protected by the LSM theorem is very similar to the boundary of a symmetry protected topological (SPT) phase^{4,5}: with certain symmetry, the boundary of the SPT state cannot be a featureless gapped state. Thus in recent years many works have made the connection between the LSM theorem and related physics in the d -dimensional space to the boundary of systems with one higher dimension⁶⁻¹², and once the lattice symmetry is viewed as an internal onsite symmetry, the LSM theorem can be interpreted as the consequence of the 't Hooft anomaly at the boundary of the higher dimensional parent SPT phase.

Recently surprising correlated physics has been discovered in different systems with Moiré superlattice, such as superconductivity and insulator at fractional fillings¹³⁻¹⁶, which motivated a series of active theoretical studies¹⁷⁻³⁹ (a consensus of the nature of the observed insulating behavior has not been reached, in the current work we assume these insulators are Mott insulators, and hence are described by a low energy effective spin-orbital model). These systems have narrow electron band width near charge neutrality, hence the interaction effects are effectively enhanced near charge neutrality.

In two systems that are microscopically rather different, *i.e.* (1) the heterostructure of trilayer graphene (TLG) and hexagonal boron nitride (hBN), and (2) twisted bilayer graphene, MIs are observed at both 1/2 and 1/4 fillings away from the charge neutral point^{13,14,16} (some of the insulating behaviors were observed under pressure); superconductivity has also been observed in

both systems doped away from the MI phases^{15,16,55}. The similar behaviors of these two systems suggest a universal description. For the twisted bilayer graphene system (TBLG), though studies based on a two-orbital electron model on an effective triangular lattice were pursued^{17,19}, concerns were raised because the triangular lattice tight binding model does not capture the band touching at the charge neutral point, which is away from the Fermi surface^{18,20,21}. But it was believed that such triangular lattice tight binding model is fully justified for the TLG/hBN heterostructure¹⁸. The similarity of the recently observed phenomena in these two systems then suggests that an analogous model may also be sufficient to describe the most interesting correlated physics observed in TBLG.

In this work we assume that the MIs at the 1/2 and 1/4 fillings can be described by a model on the effective triangular lattice, which is definitely the case (at least) for the TLG/hBN heterostructure. The charge fluctuation is frozen in the MI, thus the system effectively is described by a model of spin and orbital degrees of freedom, where the two orbitals are physically the two valleys in the original Brillouin zone of graphene. Because the valley/orbital polarization in this system is approximately conserved since large-momentum transfer is highly suppressed due to the long wave length modulation of the background potential in the Moiré structure, the system has at least one extra $U(1)_v$ symmetry, which corresponds to rotating the electrons at the two valleys with opposite phase angles. Also, as was pointed out in Ref. 18,29, the exchange interaction between the two orbitals (valleys), which would lead to an effective Hund's coupling, could be rather weak in this system, since it involves the overlap between the wave functions at the two valleys.

So the electron model of the system should at least have $U(2) \times U(1)_v \times \mathcal{T}$ symmetry, where the $U(2)$ contains the ordinary charge $U(1)$ and spin $SU(2)$ symmetry,

and \mathcal{T} is the time-reversal symmetry. If we further ignore the Hund's coupling, the electron model should have even higher internal symmetry $[U(2)_L \times U(2)_R] \rtimes \mathcal{T}$, where L and R label the two valleys, and \mathcal{T} interchanges the two valleys. When the charge degree of freedom is frozen in the MI, the symmetry of the electron model will be inherited by the effective spin-orbital model. More detailed analysis of these symmetries will be given in the next few sections. The detailed microscopic models for a weak MI are usually rather complicated and difficult to analyze (efforts of deriving such models were made in Ref. 18,34), then the symmetries and electron fillings are the only information we have without more microscopic information of the MIs, and they are the key ingredients for the analysis of LSM and anomaly related physics.

II. MOTT INSULATOR AT 1/4 FILLING

A. With Hund's coupling

The MI at 1/4 filling has exactly one electron per Moiré superlattice site. Throughout the paper we define the symmetry of the effective spin-orbital model of the MI phase as the symmetry of the operators that create local excitations without changing the filling on each site. Then the symmetry of the spin-orbital model of the MI at 1/4 filling is

$$SO(3)_s \times U(1)_v \times \mathcal{T}. \quad (1)$$

Here we assume that there is only one $SO(3)_s$ spin symmetry, as it is already sufficient to guarantee a LSM theorem in this system. On every site of the triangular lattice, there is a four dimensional Hilbert space, which forms a spin-1/2 projective representation under $SO(3)_s$, and also a projective representation under $U(1)_v \times \mathcal{T}$. We can denote this representation as $(1/2_s, 1/2_v)$. Let's clarify the meaning of the projective representation $1/2_v$. Here, we normalize the periodicity of $U(1)_v$ such that the minimal but non-trivial $U(1)_v$ charge value carried by local operators in the effective spin-orbital model (such as the operator that hops one electron from one valley to another) is set to be ± 1 . Under this periodicity, the states in the four-dimensional Hilbert space on each site carry charge $\pm \frac{1}{2}$ under $U(1)_v$, which can be viewed as a projective representation under $U(1)_v \times \mathcal{T}$. On top of this, since the 4-fold spin-orbit Hilbert space is comprised of electronic states with single occupancy, the time-reversal symmetry \mathcal{T} should square to -1 , a property the $(1/2_s, 1/2_v)$ representation of $SO(3)_s \times U(1)_v \times \mathcal{T}$ always carry in our definition.

Our goal is to interpret the system as the boundary of a three dimensional SPT state, hence it has a 't Hooft anomaly, as was discussed in other systems in Ref. 6–12. The anomaly of a system can be analyzed in pretty much any state of the system, due to the anomaly matching condition^{40,41}. We will select a Z_2 spin liquid that can in principle exist in this spin-orbital system on the

triangular lattice, and Z_2 spin liquids can be naturally constructed at the boundary of three dimensional SPT states⁴².

To construct this Z_2 spin liquid, we first introduce a four component complex bosonic “spinon” b_α on every site of the triangular moiré superlattice. b_α forms a $(1/2_s, 1/2_v)$ representation of the $SO(3)_s \times U(1)_v \times \mathcal{T}$ symmetry. We then impose a local constraint

$$\sum_{\alpha=1}^4 b_{j,\alpha}^\dagger b_{j,\alpha} = 1, \quad (2)$$

on every site j . The local constraint above will lead to a $U(1)$ gauge degree of freedom, namely b_α is not a gauge invariant operator, it couples to a dynamical $U(1)$ gauge field. Thus we expected an excitation with the $(1/2_s, 1/2_v)$ representation to be a fractionalized excitation of the MI.

Then a Z_2 spin liquid, or a Z_2 topological order can be constructed by condensing the pair of the b_α field, and b_α is the e particle of the Z_2 topological order. In the Z_2 spin liquid, besides the spinon b_α , there is also a vison excitation, which is the π -flux of the original $U(1)$ gauge field, and also the m excitation of the Z_2 topological order. The dynamics of the vison is frustrated by the spinon on every site, and its dynamics is described by a fully frustrated quantum Ising model on the dual honeycomb lattice. The vison Hamiltonian should be invariant under the spin-orbit symmetry $SO(3)_s \times U(1)_v \times \mathcal{T}$. The fully frustrated quantum Ising model should have the entire lattice symmetry such as the C_3 rotation. Hence in its Brillouin zone there are four symmetry protected minima as was previously studied in Ref. 43, and the low energy modes of the visons should be particle-hole conjugated by the time-reversal symmetry \mathcal{T} , as time-reversal will reverse the momentum of the low energy vison modes. The low energy dynamics of the vison has a large emergent symmetry which protects the degeneracy of the minima in the vison band structure, and if the vison condenses, it will drive the system into a valence bond solid (VBS) type of state that only spontaneously breaks the lattice symmetry. Due to the emergent symmetry, the ground state manifold (GMS) of the VBS state can be most conveniently embedded into a group manifold $SO(3)_m$ ⁴³.

Using the formalism developed in Ref. 44, the Z_2 spin liquid mentioned above can be captured by a mutual Chern-Simons (CS) theory:

$$\begin{aligned} \mathcal{L} = & \sum_{\alpha=1}^4 |(\partial - ia)z_\alpha|^2 + \sum_{\beta=1}^2 |(\partial - ic)v_\beta|^2 \\ & + r_z |z_\alpha|^2 + r_v |v_\beta|^2 + \frac{i}{\pi} a \wedge dc + \dots \end{aligned} \quad (3)$$

z_α is a four-component complex boson field which carries a $(1/2_s, 1/2_v)$ representation under the full spin-orbital symmetry $SO(3)_s \times U(1)_v \times \mathcal{T}$; the two-component complex boson field v_β carries a spinor representation of the $SO(3)_m$ group; Besides the action on the boson field z_α , the time-reversal symmetry also transforms

the vison field v_β and the gauge field a and c as \mathcal{T} : $v_\beta \rightarrow v_\beta^*$, $(a_0, a_1, a_2) \rightarrow (a_0, -a_1, -a_2)$, $(c_0, c_1, c_2) \rightarrow (-c_0, c_1, c_2)$. One can check that the mutual Chern-Simons (CS) theory Eq.3 is invariant under the full spin-orbital symmetry $SO(3)_s \times U(1)_v \times \mathcal{T}$ and the $SO(3)_m$ group. When z_α and v_β are both gapped ($r_z, r_v > 0$), they are the e and m excitations of a symmetric Z_2 spin liquid on the triangular lattice, with a mutual semion statistics enforced by the mutual CS term. The VBS phase mentioned in the previous paragraph which corresponds to the condensate of visons can be obtained by keeping $r_z > 0$, while bringing $r_v < 0$. Then after integrating out the gapped b_α field, the vison field v_β is coupled to a mutual CS field which is equivalent to a Z_2 gauge field, and the condensate of v_β has the ground state manifold $SO(3)_m$ which can be described by three orthogonal gauge invariant vectors⁴⁵:

$$v^\dagger \vec{\sigma} v, \quad \text{Re}[v^t \sigma^y \vec{\sigma} v], \quad \text{and} \quad \text{Im}[v^t \sigma^y \vec{\sigma} v]. \quad (4)$$

Eq. 3 is sufficient for us to “derive” the ’t Hooft anomaly. But let us first discuss the physical construction of the bulk SPT phase in three dimensions, whose boundary is the same Z_2 topological order given by Eq. 3. We will try to construct a 3d SPT phase with $SO(3)_s \times U(1)_v \times \mathcal{T} \times SO(3)_m$ onsite symmetry through the standard “decorated defect” procedure^{10,42,46}:

(1) In the 3d bulk, we first consider an ordered phase whose order parameter forms a ground state manifold $SO(3)_m$;

(2) Then in the ordered phase of the $SO(3)_m$ order parameter, due to the fact that $\pi_1[SO(3)] = Z_2$, there is a Z_2 vortex line topological excitation (defect);

(3) Then we decorate this Z_2 vortex line with the 1d SPT phase with $SO(3)_s \times U(1)_v \times \mathcal{T}$ symmetry whose boundary is a $(1/2_s, 1/2_v)$ representation;

(4) Eventually we restore all the symmetry in the bulk by proliferating/condensing the vortex loops which have been decorated with the 1d SPT phase.

To elaborate this construction, we need to review the 1d SPT phases. There is a standard 1d Haldane SPT phase with $SO(3)_s$ symmetry^{47,48} with Z_2 classification. $U(1)_v \times \mathcal{T}$ SPT state in 1d has a $Z_2 \times Z_2$ classification^{4,5,49}. There is one 1d $U(1)_v \times \mathcal{T}$ SPT state whose 0d boundary carries half charge under $U(1)_v$, and also a Kramers doublet such that the time-reversal action squares to -1 . It is the *product* of the two 1d SPT phases mentioned above that we decorate into the vortex line of the $SO(3)_m$ order parameter in the previous paragraph, which again has a Z_2 classification itself, namely two copies of this product 1d SPT phases become a trivial phase. The 0d boundary of this 1d SPT phase is precisely the $(1/2_s, 1/2_v)$ representation under the $SO(3)_s \times U(1)_v \times \mathcal{T}$ symmetry. The Z_2 nature of the vortex line of the ground state manifold $SO(3)_m$ is perfectly compatible with the Z_2 classification of the 1d SPT phase decorated along the vortex lines.

Please note that in this construction, we will proliferate the decorated closed vortex loops in the bulk, but we will

not (in fact we cannot) proliferate the “termination” of a single vortex line on the 2d boundary without breaking any symmetry, because the termination of a single vortex line at the boundary corresponds to the boundary of the 1d SPT phase, which carries a projective representation of the spin-orbital symmetry, whose condensation will lead to spontaneous breaking of the spin-orbital symmetry. However, at the 2d boundary, we can disorder the $SO(3)_m$ order parameter, while keeping a finite gap of the vortex of the $SO(3)_m$ order parameter. Then the system enters a Z_2 topological order whose e particle is the gapped vortex of the $SO(3)_m$ order parameter with a $(1/2_s, 1/2_v)$ projective representation, and the m particle is the “fractionalized” $SO(3)_m$ order parameter, which is precisely the v_β field Eq. 3, and v_β is connected to the $SO(3)_m$ order parameter through Eq. 4.

A similar Z_2 spin liquid as Eq. 3 can be naturally constructed for an ordinary spin-1/2 system on the triangular lattice, whose e and m excitations carry spin-1/2 representations of $SO(3)_s$ and $SO(3)_m$ group respectively⁴⁴. In Ref. 10,50 it was shown that there is a “parent state” of this Z_2 spin liquid, which is an algebraic spin liquid state described by the $N_f = 4$ QED₃ with four flavors of (two-component) Dirac fermions coupled with a dynamical $U(1)$ gauge field, and hence has an emergent $SU(4)$ flavor symmetry⁵⁶. The $SO(3)_s$ and $SO(3)_m$ symmetries are both subgroups of the $SU(4)$ flavor symmetry, and a spin-1/2 system on the triangular lattice can be viewed as the boundary of a 3d SPT phase with $SO(3)_s \times SO(3)_m$ symmetry. The 3d bulk SPT is constructed by decorating the vortex line of the $SO(3)_m$ manifold with a $SO(3)_s$ Haldane phase¹⁰.

It is natural to see that in the parent QED₃ state the translation symmetries of the lattice correspond to the $Z_2 \times Z_2$ subgroup of the $SO(3)_m$ group, *i.e.* they are the π -rotation around two orthogonal axes (more detail is given in the appendix). In fact, as long as we preserve the translation symmetry of the triangular lattice (but break the rotation symmetry), it is already sufficient to guarantee a LSM theorem. In this case, the system can still be viewed as the boundary of a 3d SPT state, while now the $SO(3)_m$ vortex line becomes the 1d intersection of the domain walls of the two Z_2 subgroups (Fig. 1), and the bulk is still a nontrivial 3d SPT phase once we decorating this domain wall intersection with a 1d SPT phase.

In our current case a similar QED₃ parent state can be constructed. In order to do that, we need to introduce two types of fermionic partons on each site. We introduce $f_s = (f_{s,1}, f_{s,2})^t$ that forms a spin- $\frac{1}{2}_s$ representation under $SO(3)_s$, that is charge neutral under $U(1)_v$ and has a time-reversal actions \mathcal{T} that squares to -1 . We also introduce the parton $f_v = (f_{v,1}, f_{v,2})^t$ that is a doublet consisting of modes with charge $\pm \frac{1}{2}$ under $U(1)_v$. $f_{v,1}$ and $f_{v,2}$ are interchanged under the \mathcal{T} action such that the time-reversal action squares to $+1$. f_v transform trivially under $SO(3)_s$. Then by imposing the constraint that f_v and f_s each has exactly one fermion on each site

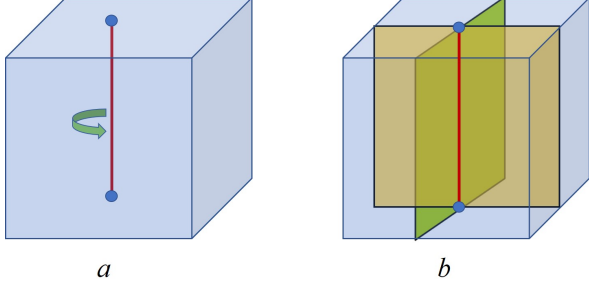


FIG. 1: (a) The “decorated defect” construction of the 3d bulk SPT state: for the MI with 1/4 filling, we decorate a 1d SPT with $SO(3)_s \times U(1)_v \times \mathcal{T}$ symmetry in every Z_2 vortex line of the $SO(3)_m$ order parameter manifold; (b) When the rotation symmetry of the triangular lattice is broken, while the translation symmetry is preserved, the translation symmetry becomes the $Z_2 \times Z_2$ subgroup of $SO(3)_m$, and the vortex line is reduced to the intersection of two Z_2 domain walls.

j :

$$\sum_{\alpha=1}^2 f_{j,s,\alpha}^\dagger f_{j,s,\alpha} = 1, \quad \sum_{\alpha=1}^2 f_{j,v,\alpha}^\dagger f_{j,v,\alpha} = 1, \quad (5)$$

the Hilbert space on each site still forms a $(1/2_s, 1/2_v)$ projective representation of the spin-orbital group $SO(3)_s \times U(1)_v \times \mathcal{T}$. Then f_s and f_v can each form a $N_f = 4$ QED₃ with two distinct dynamical $U(1)$ gauge fields, *i.e.* the parent state of the Z_2 spin liquid Eq. 3 is two copies of $N_f = 4$ QED₃.

Let us discuss the connection between the two copies of $N_f = 4$ QED₃ and the aforementioned Z_2 spin liquid. We start with the two copies of QED₃. In the $N_f = 4$ QED₃ associated to the f_s parton, the low-energy Dirac fermions, denoted as ψ_s , carry the same quantum number as the f_s parton under symmetry $SO(3)_s \times \mathcal{T}$. ψ_s also forms a doublet representation under $SO(3)_m$. Overall, the ψ_s fermion forms a $N_f = 4$ dimensional representation of the total group $SO(3)_s \times \mathcal{T} \times SO(3)_m$. The $U(1)$ gauge field that couples to ψ_s transforms in the same way as the standard electromagnetism under \mathcal{T} . In this QED₃, we can turn on a singlet pairing of the ψ_s that is invariant under the total group. This pairing higgs the $U(1)$ gauge group down to Z_2 , which indicates the Z_2 topological order in the Higgs phase. The fermion ψ_s will naturally be identified as the fermionic particle in the Z_2 topological order. There are two types of (deconfined) π -fluxes that will be identified as the “electric” and “magnetic” particles of the Z_2 topological order¹⁰. We denote them as e_1 and m_1 particles. They differ from each other by a fermion ψ_s and they have the semionic mutual statistics. The m_1 particle transforms trivially under the spin-orbital group $SO(3)_s \times \mathcal{T}$ but forms a doublet representation under $SO(3)_m$. The e_1 particle forms a spin- $\frac{1}{2}_s$ representation under $SO(3)_s$ such that the time-reversal \mathcal{T} squares to -1 . e_1 is invariant under

the $U(1)_v$ and $SO(3)_m$ actions.

In the $N_f = 4$ QED₃ associated to the f_v parton, the low-energy Dirac fermions, denoted as ψ_v , carry the same quantum number as the f_v parton under the spin-orbital symmetry group $U(1)_v \times \mathcal{T}$. ψ_v also forms a doublet representation under $SO(3)_m$. Overall, the ψ_v fermion forms a $N_f = 4$ dimensional representation of the total group $U(1)_v \times \mathcal{T} \times SO(3)_m$. Similarly, we can turn on the fermion pairing that is a singlet under the total group to deform this QED₃ into another Z_2 topological order. Again, the fermionic particle of the Z_2 topological order is naturally identified with ψ_v . The two types of (deconfined) π -fluxes can be identified as the “electric” particle e_2 and “magnetic” particle m_2 of the Z_2 topological order¹⁰. They differ from each other by a fermion ψ_v and they have mutual semionic statistics. The m_2 particle transforms trivially under the spin-orbital group $U(1)_v \times \mathcal{T}$ but again forms a doublet representation under $SO(3)_m$. The e_2 particle forms a doublet with $\pm \frac{1}{2}$ $U(1)_v$ charges. The two components of the e_2 doublet are interchanged by the time-reversal symmetry \mathcal{T} such that the time-reversal symmetry square to 1 on e_2 . e_2 is invariant under the $SO(3)_s$ and $SO(3)_m$ actions.

Now we have constructed two copies of Z_2 topological order with the quasi-particle contents $\{1, e_1, m_1, \psi_s\}$ and $\{1, e_2, m_2, \psi_v\}$ where 1 stands for the trivial particle. Since m_1 and m_2 are both doublets under the $SO(3)_m$ group, we can further condense the pair $m_1 m_2$ which is a singlet under $SO(3)_m$ without breaking any symmetry. The resulting topological order is a single copy of Z_2 topological order whose electric particle can be identified as $e_1 e_2$ and magnetic particle as m_1 (which is equivalent to m_2). One can immediately check that the deconfined particle $e_1 e_2$ (which has a trivial braiding statistics with the condensed bound state $m_1 m_2$) has the same statistics and symmetry quantum numbers as the boson field z_α in the Z_2 spin liquid phase of Eq. 3. Also, the particle m_1 has the same statistics and symmetry quantum numbers as the vison field v_β in the Z_2 spin liquid phase of Eq. 3. Now, we can conclude that we have constructed the Z_2 spin liquid phase of the mutual CS theory Eq. 3 from the two copies of $N_f = 4$ QED₃.

As we discussed, this Z_2 spin liquid should be the boundary state of a 3d SPT phase with $SO(3)_s \times U(1)_v \times \mathcal{T} \times SO(3)_m$ that can be described using the “decorated-defect” construction. From the construction of this 3d SPT, we can directly write down its topological response action

$$\mathcal{S} = \pi \int (w_2[\mathcal{A}_s] + \frac{1}{2\pi} dA_v + w_1^2[TM]) \cup w_2[\mathcal{A}_m] \quad (6)$$

under the background $SO(3)_s$ gauge field \mathcal{A}_s , $SO(3)_m$ gauge field \mathcal{A}_m , $U(1)_v$ gauge field A_v and tangent bundle TM of spacetime manifold. Here, $w_{1,2}$ stand for the first and the second Stiefel-Whitney classes. In this topological response action, the $w_2[\mathcal{A}_m]$ part physically measures the $SO(3)_m$ flux. The $w_2[\mathcal{A}_s]$ term captures the topological response of the 1d $SO(3)_s$ Haldane chain. The dA_v

term describes a $1d$ SPT with a half $U(1)_v$ charge, which is protected by \mathcal{T} , on its boundary. The $w_1^2[TM]$ term characterizes a $1d$ SPT with a Kramers doublet (such that the time-reversal action squares to -1) on its boundary. This topological response implies non-trivial 't Hooft anomaly on the boundary state of this $3d$ SPT, which in this case can be further viewed as an implication of the LSM theorem in the effective spin-orbital model on the Moiré superlattice site with filling $\frac{1}{4}$. From the topological action, we see that the 't Hooft anomaly (and hence the LSM theorem) should exist even if we consider only the $SO(3)_s \times SO(3)_m$ symmetry or only the symmetry $\mathcal{T} \times SO(3)_m$, where $SO(3)_m$ essentially represents the space-group symmetry that at least includes the lattice translation symmetries. This means that even if we break the $SO(3)_s$ and $U(1)_v$, as long as \mathcal{T} and translation is still preserved, there is still a LSM theorem for this system, and the system can still be viewed as the boundary of a nontrivial $3d$ SPT state.

B. Without Hund's coupling

Now let us consider the case where the Hund's coupling is ignored, which is justified in some limit since as we argued before in this system the Hund's coupling is supposed to be weak. In this case operators that create local excitations form a linear representation of $SO(4)_s = [SU(2)_L \times SU(2)_R]/Z_2$, where $SU(2)_L$ and $SU(2)_R$ are spin symmetries on the left and right valleys respectively. Hence in this case the symmetry of this MI is just $SO(4)_s \rtimes \mathcal{T} \times U(1)_v$. The \rtimes symbol stems from the fact that time-reversal interchanges the two $SU(2)$ subgroups, hence time-reversal acts like an improper rotation.

Every site of the Moiré lattice carries a Dirac spinor projective representation of the $SO(4)_s$ symmetry group, *i.e.* a $(1/2, 0) \oplus (0, 1/2)$ representation. A Z_2 topological order can still be constructed in this system like Eq. 3, while in this case b_α is a Dirac spinor of $SO(4)_s$, and also a projective representation of $U(1)_v \times \mathcal{T}$. In fact, we can also embed the $SO(4)_s$ and $U(1)_v$ into a $SO(6)_s$ group, and the four dimensional Hilbert space forms a spinor of the enlarged $SO(6)_s$ symmetry.

The construction of the $3d$ bulk SPT phase is similar as before. We can decorate the Z_2 vortex line of the $SO(3)_m$ order parameter manifold with a $1d$ SPT phase whose $1d$ bulk has a vector representation of $SO(4)_s$ and also a linear representation of $U(1)_v \times \mathcal{T}$, while its $0d$ boundary has a Dirac spinor of $SO(4)_s$ and a projective representation of $U(1)_v \times \mathcal{T}$. This $1d$ SPT phase itself still has a Z_2 classification, which is consistent with the Z_2 vortex line of the $SO(3)_m$ order parameter manifold. Then the natural boundary of this $3d$ SPT state is still the Z_2 topological order described above.

III. MOTT INSULATOR AT 1/2 FILLING

Weak MI behavior was also discovered at $1/2$ filling doped away from charge neutrality, in both TLG/hBN heterostructure and twisted bilayer graphene^{13,14,16}. The $1/2$ filling means that there are two extra electrons/holes per unit cell away from charge neutrality in the Moiré superlattice. If we use a triangular lattice model to describe these systems, then for the twisted bilayer graphene, the symmetry of the system guarantees that the nearest neighbor hopping of the electrons has a $U(4)$ symmetry, while the $U(4)$ to $U(2)_L \times U(2)_R$ symmetry breaking will happen only in second neighbor hopping, as the symmetry permits a valley dependent imaginary hopping between second neighbor sites; for the TLG/hBN heterostructure, the valley dependent imaginary hopping is permitted even between the nearest neighbor sites¹⁸.

Let us first start with the $U(4)$ limit of the systems. When the charge degree of freedom is completely frozen, the system will be described by a $SU(4) \sim SO(6)$ spin model with a six component vector representation on every site. Under the $U(4)$ to $U(2)_L \times U(2)_R$ symmetry breaking, the six states on every site will be split into a four component $SO(4) \sim [SU(2)_L \times SU(2)_R]/Z_2$ vector, and two degenerate $SO(4)$ singlet states. Thus there are two possible scenarios: the microscopic Hamiltonian either prefers the four component $SO(4)$ vector states, or the two component $SO(4)$ singlet states. In the following we will study each scenario separately. If the Hund's coupling is considered, then at least the former case has a spin-1 left on every site, which no longer has a LSM theorem. In principle one can construct a featureless spin state by splitting each spin-1 into three spin-1 objects, and each of these "fractionalized" spin-1 object forming a Haldane chain along one of the three directions of the triangular lattice. Thus in this section we will ignore the Hund's coupling, *i.e.* we assume there is no exchange interaction between the two valleys.

A. $SO(4)$ vector state on each site

Let us first consider the case where the microscopic Hamiltonian prefers to have a four-component vector states on each site of the triangular moiré superlattice. In fact, we will consider the limit where the two other states of the $SO(6)$ vector is completely projected out. Physically, this case implies that the microscopic Hamiltonian favors to have one and exact one electron each valley (orbital) on every site.

A more careful analysis of the symmetry of the MI is necessary. It is crucial to distinguish the symmetry of the electron system, and the symmetry of the low energy effective spin model that describes the MI. As we mentioned before, the electron symmetry is $[U(2)_L \times U(2)_R] \rtimes \mathcal{T}$. However, the symmetry of the spin model should be identified as the symmetry carried by the creation operators of local spin excitations. For example, for an ordi-

nary spin system, whether it has integer or half-integer spin in each unit cell, the local spin excitations always carry integer spins, thus the local spin creation operators always have $SO(3)$ spin symmetry, and a spin-1/2 excitation can only be “fractionalized”. Using this perspective, under the assumption that there is always one and precisely one electron on each valley, the precise symmetry of the allowed local operators which create spin excitations is

$$[SO(3)_L \otimes SO(3)_R] \rtimes \mathcal{T} = pSO(4)_s \rtimes \mathcal{T}. \quad (7)$$

This symmetry group needs some explanation. Since we have projected the onsite Hilbert space on one electron on each valley, an allowed local excitation cannot mix the two valleys, *i.e.* it cannot move an electron from one valley to another. So an local spin operator will take the form $c_L^\dagger \vec{\sigma} c_L$, or $c_R^\dagger \vec{\sigma} c_R$, both form linear representations of $SO(3)_L \otimes SO(3)_R$.

$pSO(4)$ is the $SO(4)$ group mod out its Z_2 center. Let us recall that $SO(4) = [SU(2) \otimes SU(2)]/Z_2$, where the Z_2 in the “denominator” is the common Z_2 center of the two $SU(2)$ subgroups, *i.e.* the simultaneous 2π rotation of both $SU(2)$ becomes the identity element in $SO(4)$. In $pSO(4)$ we need to mod out another Z_2 subgroup, because as we discussed above, the local spin excitation of the system must carry linear representation of both $SO(3)_L$ and $SO(3)_R$, while a vector representation of the original $U(2)_L \times U(2)_R$ electron symmetry is now a projective representation of the spin symmetry $pSO(4)$. Hence a four component $SO(4)$ vector spin excitation can only be a “fractionalized” excitation of the spin system, and can only exist in a “spin liquid”.

The time-reversal symmetry \mathcal{T} exchanges the two valleys. Since the effective spin model Hilbert space on each site consists of states with two electrons each site, the square of the \mathcal{T} action on the effective spin Hilbert space is +1 (instead of -1 as in the $\frac{1}{4}$ filling case). The $U(1)_v$ acts completely trivially both on the operators and the spin states in this effective spin model. Hence, we don’t need to include $U(1)_v$ in the discussion that follows.

As before, in order to expose the anomaly of the system, we can construct a similar Z_2 spin liquid as Eq. 3. We first define a four component complex bosonic “spinon” b_α on every site of the triangular moiré superlattice, b_α forms a $(1/2, 1/2)$ representation under the $U(2)_L \times U(2)_R$ electron symmetry, or a vector (projective) representation of the $pSO(4)_s$ spin symmetry. The time-reversal symmetry \mathcal{T} squares to 1 on the boson field b_α . We then impose a local constraint $\sum_{\alpha=1}^4 b_{j,\alpha}^\dagger b_{j,\alpha} = 1$, on every site j . Then a Z_2 spin liquid, or a Z_2 topological order can be constructed by condensing the pair of the b_α field, and b_α is the e particle of the Z_2 topological order. The vison field v_β still forms a spin-1/2 representation of the $SO(3)_m$ group.

This Z_2 spin liquid can again be viewed as the boundary of a 3d SPT phase. To elaborate this bulk construction, we need to review the 1d SPT phases with the $pSO(4)_s = SO(3)_L \times SO(3)_R$ symmetry. These

1d SPT phases have classification $Z_2 \times Z_2$ ⁵¹. The two “root” states are basically the Haldane phase of $SO(3)_L$ and $SO(3)_R$ respectively, *i.e.* its boundary carries either $(1/2, 0)$ or $(0, 1/2)$ projective representation of $pSO(4)_s$. Then the SPT phase with a vector representation $(1/2, 1/2)$ at the boundary is a product of both root states, and itself has a Z_2 classification, namely two copies of this SPT phases will trivialize themselves. It is this product SPT phase that we decorate into the vortex line of a $SO(3)_m$ order parameter in the bulk, and this product SPT phase preserves the Z_2 improper rotation of the $pSO(4)_s$ symmetry that exchanges $SO(3)_L$ and $SO(3)_R$, thus it also preserves the time-reversal which acts as the improper rotation. Here, notice that, unlike the $\frac{1}{4}$ filling case, we do NOT decorate the $SO(3)_m$ vortex line by the 1d SPT state with a time-reversal Kramers doublet on its boundary. This is because the time-reversal action squares to -1 on a Kramers doublet, which is incompatible with the representation of the boson field b_α or the effective spin Hilbert space on each site.

From the decorated-defect construction of this 3d SPT, we can write down its topological response action

$$\mathcal{S} = \pi \int (w_2[\mathcal{A}_L] + w_2[\mathcal{A}_R]) \cup w_2[\mathcal{A}_m] \quad (8)$$

under the background $SO(3)_L$ gauge field \mathcal{A}_L , $SO(3)_R$ gauge field \mathcal{A}_R and $SO(3)_m$ gauge field \mathcal{A}_m . This topological response action indicates the non-trivial ’t Hooft anomaly on the boundary of this 3d SPT phase which can be further interpreted as the LSM theorem on the Moiré superlattice site with filling $\frac{1}{2}$ (under the $pSO(4)_s \rtimes \mathcal{T} \times SO(3)_m$ symmetry). If we further turn on the Hund’s coupling in this effective model, the $SO(3)_L \times SO(3)_R$ symmetry is broken down to its diagonal subgroup. In the topological response theory, it amounts to setting $\mathcal{A}_L = \mathcal{A}_R$. Since w_2 is a cohomology class with Z_2 coefficient, the topological response theory becomes trivial when $\mathcal{A}_L = \mathcal{A}_R$. Hence, the LSM theorem does not exist when the Hund’s rule coupling is turned on, which we expected before.

B. $SO(4)_s$ singlet state on each site

Now let us consider the case where the microscopic onsite Hamiltonian strongly prefers two electrons on either the left or right valley, hence it is a singlet under either $SU(2)_L$ or $SU(2)_R$ electron symmetry. We will use $\tau^z = \pm 1$ to label the two states with fully occupied left and right valleys respectively, and the $U(1)_v$ transformation rotates the left and right valleys by an opposite phase angle. The $U(1)_v$ symmetry corresponds to the conservation of electron number on each valley separately, which is a justified emergent symmetry at low energy.

Under time-reversal \mathcal{T} , τ^z changes its sign, thus the symmetry in the two dimensional spin singlet Hilbert

space is $U(1)_v \times \mathcal{T}$. Here, we normalize the periodicity of the $U(1)_v$ group such that the a local operator of this low energy effective model (for example the operator that hops two electrons on the left valley to the right valley) always carry integer charge under $U(1)_v$. Under this normalization, the two states on each site of this effective models carry $\pm \frac{1}{2} U(1)_v$ charge. Under \mathcal{T} , the two states on each site are exchanged. This time-reversal action on the quantum states squares to 1. A Z_2 topological order can still be constructed in this case, which is also described by Eq. 3, the only difference is that $\alpha = 1, 2$ in the first term of the Lagrangian, and z_α transforms as a projective representation of $U(1)_v \times \mathcal{T}$. The dynamics of the vison is unchanged from Eq. 3.

This system again has a LSM theorem, *i.e.* it cannot have fully gapped nondegenerate ground state without breaking the $U(1)_v \times \mathcal{T}$ symmetry. We can also map this system to the boundary of a 3d SPT phase. The construction is similar to the previous subsection: we consider the ordered phase in the 3d bulk with ground state manifold $SO(3)_m$; then we decorate this Z_2 vortex line with the 1d SPT phase with $U(1)_v \times \mathcal{T}$ symmetry whose boundary is a projective representation of $U(1)_v \times \mathcal{T}$; eventually we restore the symmetry in the bulk by proliferating the vortex loops. From the decorated-defect construction of this 3d SPT, we can write down its topological response action

$$\mathcal{S} = \pi \int \frac{1}{2\pi} A_v \cup w_2[\mathcal{A}_m] \quad (9)$$

under the background $U(1)_v$ gauge field A_v and $SO(3)_m$ gauge field \mathcal{A}_m . The coefficient π in the topological response theory is protected by \mathcal{T} . Similar to the previous discussions, this topological response action is tied to the non-trivial LSM theorem.

IV. DISCUSSION

Given the novel effective symmetry groups of the moiré systems discovered recently, we have analyzed possible spin-orbital states of the weak Mott insulators observed at both 1/2 and 1/4 fillings away from the charge neutrality. Due to the weak charge gap of the MIs, the detailed effective spin-orbital Hamiltonian for these MIs is expected to be rather complicated, thus in our paper we focused on general analysis that only relies on the uni-

versal information such as symmetry and electron filling. We mapped the MIs to the boundary of 3d SPT phases, and demonstrated the 't Hooft anomaly which is associated with the LSM theorem.

The two different moiré systems (TLG/hBN and TBLG) have different detailed lattice symmetries such as reflection, inversion, etc. Thus in our paper we focused on the common symmetries shared by both systems. It is known that the 't Hooft anomaly at the boundary of a 3d SPT state is usually related to the deconfined quantum critical point^{7,8,10,42,52–54}, and the novel symmetries in the moiré systems may support new types of deconfined quantum critical points awaiting experimental findings. We will leave this potentially exciting explorations to future studies.

Chao-Ming Jian's research at KITP is supported by the Gordon and Betty Moore Foundations EPiQS Initiative through Grant GBMF4304. Cenke Xu is supported by the David and Lucile Packard Foundation.

Appendix A: Parton construction for the $N_f = 4$ QED₃

This section focuses on the parton construction, following Ref. 50, of the $N_f = 4$ QED₃ for the parton f_s and f_v discussed in Sec. II A. Take the f_s parton as an example. There are two fermion modes $f_{s,\alpha}$ with $\alpha = 1, 2$ at each site. We impose the constraint that there is exactly one f_s fermion/parton per site. In another words, this constraint enforces the half filling of the f_s fermions. In the following, we will suppress the subscript “s” to simplify the notation. In the following, we will consider a mean-field ansatz that does not depend on the mode index $\alpha = 1, 2$. Hence, we will also suppress the subscript α for simplicity. The mean-field ansatz we consider corresponds to the π -flux phase where we insert a π flux in every down triangle. In this π -flux phase, we only include the nearest-neighbor hopping that takes value t along the black edges and $-t$ along the red edges as is shown in Fig. 2 (a). A Bloch unit cell in this ansatz contains 4 sites. We choose the convention such that the 4 blue sites in Fig. 2 (a) form a unit cell. The four fermions within a unit cell are organized into a 4-component spinor according to the ordering shown in Fig. 2 (b). The parton mean-field band structure is given by the Bloch Hamiltonian

$$H_{\text{mf}}(k_1, k_2) = t \begin{pmatrix} 0 & 1 + e^{ik_2 - ik_1} & -1 + e^{ik_2} & e^{ik_2} (1 + e^{-ik_1}) \\ 1 + e^{ik_1 - ik_2} & 0 & -1 - e^{ik_1} & 1 - e^{ik_2} \\ -1 + e^{-ik_2} & -1 - e^{-ik_1} & 0 & 1 + e^{ik_2 - ik_1} \\ e^{-ik_2} (1 + e^{ik_1}) & 1 - e^{-ik_2} & 1 + e^{ik_1 - ik_2} & 0 \end{pmatrix}, \quad (A1)$$

where k_1 and k_2 are defined by the phases e^{ik_1} and e^{ik_2} obtained from translating the Bloch wave by one unit

cell along the a_1 and a_2 directions (see Fig. 2(a)). The

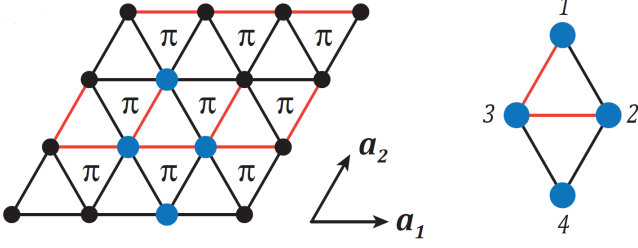


FIG. 2: (a) In the π -flux phase, we consider the mean-field with only nearest-neighbor hopping. The hopping term takes value t along the black edges and $-t$ along the red edges. We choose a convention such that the four blue sites form a unit cell. (b) We provide an ordering of the sites within a unit cell for the construction of the Bloch Hamiltonian.

translation $T_{1,2}$ by one site along a_1 and a_2 directions need to be followed by gauge transformations to keep the Hamiltonian $H_{\text{mf}}(k_1, k_2)$ invariant. The actions of $T_{1,2}$ on the 4-component spinor are given by

$$U_{T_1} = \begin{pmatrix} 0 & 0 & 0 & e^{-ik_1+ik_2} \\ 0 & 0 & 1 & 0 \\ 0 & e^{-ik_1} & 0 & 0 \\ e^{-ik_2} & 0 & 0 & 0 \end{pmatrix},$$

$$U_{T_2} = i \begin{pmatrix} 0 & 0 & -i & 0 \\ 0 & 0 & 0 & -i \\ ie^{-ik_2} & 0 & 0 & 0 \\ 0 & ie^{-ik_2} & 0 & 0 \end{pmatrix}. \quad (\text{A2})$$

The mean-field band structure given by Eq. A1 has a Dirac crossing at $(k_1, k_2) = (\pi, 0)$ at half filling, namely one f fermion per-site. We can study the low-energy

physics at the Dirac crossing by considering $(k_1, k_2) = (\pi + q_1, q_2)$ and expanding to the leading order of $q_{1,2}$. We can also switch to the Cartesian coordinates (q_x, q_y) defined by the relation $(q_1, q_2) = (q_x, \frac{1}{2}q_x + \frac{\sqrt{3}}{2}q_y)$. One can show that, under a certain basis transformation W , the leading order mean-field Bloch Hamiltonian reads:

$$W^\dagger H_{\text{mf}} W = \sqrt{\frac{3}{2}}t (q_x \sigma^{0y} + q_y \sigma^{0x}) + \dots, \quad (\text{A3})$$

where “...” stands for terms that contain higher powers of q_x and q_y . Here, we’ve used the notation $\sigma^{ab} \equiv \sigma^a \otimes \sigma^b$. σ^0 represents the 2×2 identity matrix. We notice that the leading order Hamiltonian $W^\dagger H_{\text{mf}} W$ describes two copies of Dirac fermions that form together a doublet under an emergent $SO(3)$ symmetry generated by σ^{x0}, σ^{y0} and σ^{z0} . We can also extract the leading order terms of the translation symmetry action $U_{T_{1,2}}$:

$$W^\dagger U_{T_1} W = i\sigma^{z0}, \quad W^\dagger U_{T_2} W = -i\sigma^{y0}, \quad (\text{A4})$$

which naturally corresponds to a $Z_2 \times Z_2$ subgroup of the emergent $SO(3)$ symmetry. This emergent $SO(3)$ symmetry is exactly the $SO(3)_m$ group discussed in the main text. The low-energy Dirac fermion forms a doublet under $SO(3)_m$. Remember we have suppressed the mode index $\alpha = 1, 2$ throughout the discussion. Hence, there are in fact in total 4 copies of Dirac fermions. These Dirac fermions also couple to a dynamical $U(1)$ gauge field that enforces the constraint on one f fermion per site. Hence, the π -flux phase can be described by the $N_f = 4$ QED₃.

- ¹ E. H. Lieb, T. D. Schultz, and D. C. Mattis, Ann. Phys. **16**, 407 (1961).
- ² M. Oshikawa, Phys. Rev. Lett. **84**, 1535 (2000), URL <https://link.aps.org/doi/10.1103/PhysRevLett.84.1535>.
- ³ M. B. Hastings, Phys. Rev. B **69**, 104431 (2004), URL <http://link.aps.org/doi/10.1103/PhysRevB.69.104431>.
- ⁴ X. Chen, Z.-C. Gu, Z.-X. Liu, and X.-G. Wen, Phys. Rev. B **87**, 155114 (2013).
- ⁵ X. Chen, Z.-C. Gu, Z.-X. Liu, and X.-G. Wen, Science **338**, 1604 (2012).
- ⁶ S. C. Furuya and M. Oshikawa, Phys. Rev. Lett. **118**, 021601 (2017), URL <https://link.aps.org/doi/10.1103/PhysRevLett.118.021601>.
- ⁷ C.-M. Jian, Z. Bi, and C. Xu, Phys. Rev. B **97**, 054412 (2018), URL <https://link.aps.org/doi/10.1103/PhysRevB.97.054412>.
- ⁸ M. A. Metlitski and R. Thorngren, Phys. Rev. B **98**, 085140 (2018), URL <https://link.aps.org/doi/10.1103/PhysRevB.98.085140>.
- ⁹ G. Y. Cho, C.-T. Hsieh, and S. Ryu, Phys. Rev. B **96**, 195105 (2017), URL <https://link.aps.org/doi/10.1103/PhysRevB.96.195105>.

- ¹⁰ C.-M. Jian, A. Thomson, A. Rasmussen, Z. Bi, and C. Xu, Phys. Rev. B **97**, 195115 (2018), URL <https://link.aps.org/doi/10.1103/PhysRevB.97.195115>.
- ¹¹ Y. Yao, C.-T. Hsieh, and M. Oshikawa, arXiv:1805.06885 (2018).
- ¹² M. Cheng, arXiv:1804.10122 (2018).
- ¹³ G. Chen, L. Jiang, S. Wu, B. Lv, H. Li, K. Watanabe, T. Taniguchi, Z. Shi, Y. Zhang, and F. Wang, arXiv:1803.01985 (2018).
- ¹⁴ Y. Cao, V. Fatemi, A. Demir, S. Fang, S. L. Tomarken, J. Y. Luo, J. D. Sanchez-Yamagishi, K. Watanabe, T. Taniguchi, E. Kaxiras, et al., Nature **556**, 80 (2018).
- ¹⁵ Y. Cao, V. Fatemi, S. Fang, K. Watanabe, T. Taniguchi, E. Kaxiras, and P. Jarillo-Herrero, Nature **556**, 43 (2018).
- ¹⁶ M. Yankowitz, S. Chen, H. Polshyn, K. Watanabe, T. Taniguchi, D. Graf, A. F. Young, and C. R. Dean, arXiv:1808.07865 (2018).
- ¹⁷ C. Xu and L. Balents, Phys. Rev. Lett. **121**, 087001 (2018), URL <https://link.aps.org/doi/10.1103/PhysRevLett.121.087001>.
- ¹⁸ H. C. Po, L. Zou, A. Vishwanath, and T. Senthil, arXiv:1803.09742 (2018).

- ¹⁹ J. F. Dodaro, S. A. Kivelson, Y. Schattner, X. Q. Sun, and C. Wang, Phys. Rev. B **98**, 075154 (2018), URL <https://link.aps.org/doi/10.1103/PhysRevB.98.075154>.
- ²⁰ N. F. Q. Yuan and L. Fu, Phys. Rev. B **98**, 045103 (2018), URL <https://link.aps.org/doi/10.1103/PhysRevB.98.045103>.
- ²¹ J. Kang and O. Vafeek, arXiv:1805.04918 (2018).
- ²² B. Padhi, C. Setty, and P. W. Phillips, Nano Letters **18**, 6175 (2018), pMID: 30185049, <https://doi.org/10.1021/acs.nanolett.8b02033>, URL <https://doi.org/10.1021/acs.nanolett.8b02033>.
- ²³ B. Padhi and P. Phillips, arXiv:1810.00884 (2018).
- ²⁴ T. Huang, L. Zhang, and T. Ma, arXiv:1804.06096 (2018).
- ²⁵ C.-C. Liu, L.-D. Zhang, W.-Q. Chen, and F. Yang, arXiv:1804.10009 (2018).
- ²⁶ L. Rademaker and P. Mellado, arXiv:1805.05294 (2018).
- ²⁷ H. Isobe, N. F. Q. Yuan, and L. Fu, arXiv:1805.06449 (2018).
- ²⁸ M. Koshino, N. F. Q. Yuan, T. Koretsune, M. Ochi, K. Kuroki, and L. Fu, Phys. Rev. X **8**, 031087 (2018), URL <https://link.aps.org/doi/10.1103/PhysRevX.8.031087>.
- ²⁹ Y.-Z. You and A. Vishwanath, arXiv:1805.06867 (2018).
- ³⁰ F. Wu, A. H. MacDonald, and I. Martin, arXiv:1805.08735 (2018).
- ³¹ G.-Y. Zhu, T. Xiang, and G.-M. Zhang, arXiv:1806.07535 (2018).
- ³² B. Lian, Z. Wang, and B. A. Bernevig, arXiv:1807.04382 (2018).
- ³³ H. Guo, X. Zhu, S. Feng, and R. T. Scalettar, Phys. Rev. B **97**, 235453 (2018), URL <https://link.aps.org/doi/10.1103/PhysRevB.97.235453>.
- ³⁴ Y.-H. Zhang and T. Senthil, arXiv:1809.05110 (2018).
- ³⁵ H. C. Po, L. Zou, T. Senthil, and A. Vishwanath, arXiv:1808.02482 (2018).
- ³⁶ Q. K. Tang, L. Yang, D. Wang, F. C. Zhang, and Q. H. Wang, arXiv:1809.06772 (2018).
- ³⁷ A. Thomson, S. Chatterjee, S. Sachdev, and M. S. Scheurer, Phys. Rev. B **98**, 075109 (2018), URL <https://link.aps.org/doi/10.1103/PhysRevB.98.075109>.
- ³⁸ K. Hejazi, C. Liu, H. Shapourian, X. Chen, and L. Balents, arXiv:1808.01568 (2018).
- ³⁹ J. Liu, J. Liu, and X. Dai, arXiv:1810.03103 (2018).
- ⁴⁰ G. 't Hooft, *Recent Developments in Gauge Theories*, (Plenum Press, New York; reprinted in “Unity of Forces in the Universe”, edited by A. Zee (World Scientific, Singapore, 1982), Vol. II, p. 1004., 1980).
- ⁴¹ A. Zee, Physics Letters B **95**, 290 (1980).
- ⁴² A. Vishwanath and T. Senthil, Phys. Rev. X **3**, 011016 (2013).
- ⁴³ R. Moessner and S. L. Sondhi, Phys. Rev. B **63**, 224401 (2001), URL <https://link.aps.org/doi/10.1103/PhysRevB.63.224401>.
- ⁴⁴ C. Xu and S. Sachdev, Phys. Rev. B **79**, 064405 (2009), URL <https://link.aps.org/doi/10.1103/PhysRevB.79.064405>.
- ⁴⁵ A. V. Chubukov, S. Sachdev, and T. Senthil, Nuclear Physics B **426**, 601 (1994), ISSN 0550-3213, URL <http://www.sciencedirect.com/science/article/pii/055032139490023X>.
- ⁴⁶ Z. Bi, A. Rasmussen, and C. Xu, Phys. Rev. B **91**, 134404 (2015).
- ⁴⁷ F. D. M. Haldane, Phys. Lett. A **93**, 464 (1983).
- ⁴⁸ F. D. M. Haldane, Phys. Rev. Lett. **50**, 1153 (1983).
- ⁴⁹ X.-G. Wen, Phys. Rev. B **91**, 205101 (2015), 1410.8477.
- ⁵⁰ Y.-M. Lu, Phys. Rev. B **93**, 165113 (2016), 1505.06495.
- ⁵¹ K. Duivenvoorden and T. Quella, Phys. Rev. B **87**, 125145 (2013), URL <http://link.aps.org/doi/10.1103/PhysRevB.87.125145>.
- ⁵² T. Senthil, A. Vishwanath, L. Balents, S. Sachdev, and M. P. A. Fisher, Science **303**, 1490 (2004).
- ⁵³ T. Senthil, L. Balents, S. Sachdev, A. Vishwanath, and M. P. A. Fisher, Phys. Rev. B **70**, 144407 (2004).
- ⁵⁴ C. Wang, A. Nahum, M. A. Metlitski, C. Xu, and T. Senthil, Phys. Rev. X **7**, 031051 (2017), URL <https://link.aps.org/doi/10.1103/PhysRevX.7.031051>.
- ⁵⁵ The superconductivity in the heterostructure of TLG/hBN was confirmed through private communication with Feng Wang.
- ⁵⁶ More precisely the symmetry is $SO(6) \sim SU(4)/Z_2$, because the Z_4 center of the $SU(4)$ flavor symmetry is gauged, while the gauge neutral monopole of the gauge field, which is also a physical operator, carries a vector representation of $SO(6)$.